

## Modeling cover cracking due to rebar corrosion in RC members

Satish B. Allampallewar<sup>†</sup>

*Basic Engineering Department, Maharashtra Academy of Engineering, Alandi, Pune 412105, India*

A. Srividya<sup>‡</sup>

*Civil Engineering Department, Indian Institute of Technology Bombay, Powai, Mumbai 400076, India*

*(Received May 14, 2008, Accepted November 10, 2008)*

**Abstract.** Serviceability and durability of the concrete members can be seriously affected by the corrosion of steel rebar. Carbonation front and or chloride ingress can destroy the passive film on rebar and may set the corrosion (oxidation process). Depending on the level of oxidation (expansive corrosion products/rust) damage to the cover concrete takes place in the form of expansion, cracking and spalling or delamination. This makes the concrete unable to develop forces through bond and also become unprotected against further degradation from corrosion; and thus marks the end of service life for corrosion-affected structures. This paper presents an analytical model that predicts the weight loss of steel rebar and the corresponding time from onset of corrosion for the known corrosion rate and thus can be used for the determination of time to cover cracking in corrosion affected RC member. This model uses fully the thick-walled cylinder approach. The gradual crack propagation in radial directions (from inside) is considered when the circumferential tensile stresses at the inner surface of intact concrete have reached the tensile strength of concrete. The analysis is done separately with and without considering the stiffness of reinforcing steel and rust combine along with the assumption of zero residual strength of cracked concrete. The model accounts for the time required for corrosion products to fill a porous zone before they start inducing expansive pressure on the concrete surrounding the steel rebar. The capability of the model to produce the experimental trends is demonstrated by comparing the model's predictions with the results of experimental data published in the literature. The effect of considering the corroded reinforcing steel bar stiffness is demonstrated. A sensitivity analysis has also been carried out to show the influence of the various parameters. It has been found that material properties and their inter-relations significantly influence weight loss of rebar. Time to cover cracking from onset of corrosion for the same weight loss is influenced by corrosion rate and state of oxidation of corrosion product formed. Time to cover cracking from onset of corrosion is useful in making certain decisions pertaining to inspection, repair, rehabilitation, replacement and demolition of RC member/structure in corrosive environment.

**Keywords:** Concrete; Corrosion; Modulus of Elasticity; Expansive; Cracking.

---

<sup>†</sup> Assistant Professor, Corresponding author, E-mail: [asatish@iitb.ac.in](mailto:asatish@iitb.ac.in), [sallampallewar@yahoo.co.in](mailto:sallampallewar@yahoo.co.in)

<sup>‡</sup> Associate Professor

## 1. Introduction

Steel rebar corrosion is the dominant cause of premature deterioration of RC member. Almost all forms of deterioration in RC involve ingress of deleterious fluids through the pore structure of the concrete. The alkaline passive film on steel rebar at the steel-to-concrete interface and the density of the surrounding concrete provide protection against corrosion inducing agents. The two processes mainly responsible for destruction of the alkaline passive film on steel rebar are the carbonation of concrete cover and chloride ingress through the concrete cover. Corrosion will start once the passive film of iron oxides at the steel-to-concrete interface breaks down, in presence of moisture and oxygen. Damage to the cover concrete takes place in the form of expansion, cracking and the spalling or delamination; and for steel rebar loss of bond between rebar and concrete, and loss of rebar cross-sectional area thus marks the end of service life for corrosion affected structure. Corroded steel rebar has inability to develop forces through bond and also is no longer protected against further degradation from corrosion. Deterioration of RC member affects aesthetic and cause loss of serviceability, stiffness and strength; and thus promotes premature failure. Time to cover cracking from onset of corrosion is useful in making certain cost-effective decisions pertaining to the monitoring inspections and control of corrosion, repair, rehabilitate, replace and/demolition of RC member/structure in corrosive environment. It is necessary that analytical models be developed to assess the effect of steel rebar corrosion in RC member deterioration which is capable of reproducing the experimental and or in life service trend and which will be providing the reasonable prediction of the time to cracking/safe residual service life of existing RC structure/service life of new RC structure/to design a new structure for required service life. Due to complexity of corrosion process (electrochemical), and strongly dependant on environmental factors (temperature, relative humidity, rainfall) and assumed properties of materials, measured corrosion rate/rate of corrosion process, different code specified inter relations of material properties and theoretical approach used for the analysis; predicted values from literature analytical models shown some discrepancy with the observed data from the field/laboratory.

The analysis of thin cylinders is simplified considerably by assuming constant stress over the thickness. A cylinder is considered as thin when internal diameter is more than twenty times its wall thickness. For considered corrosion problem this condition never exists. So it may not be reasonable to use thin cylindrical approach for rebar corrosion in concrete. Also some of the other reasons imposing restrictions on the application of the thin cylinder theory are: (i) the internal pressure required to burst the cylinder is twice the cracking stress of concrete if cover equal to reinforcing bar diameter is provided. If provided cover is more then requirement of internal pressure to burst the wall of concrete cylinder will be more. From thick cylinder theory maximum circumferential stress is at the inner surface of cylinder and is always numerically greater than the internal pressure. (ii) Concrete elastic modulus (the ratio between the applied stress and instantaneous strain within an assumed proportional limit) is about seven times lesser than steel (Liu and Weyers 1998). (iii) Concrete is a quasi-brittle material and behaves differently in tension and compression states because of the transition zone that exists between large particles of aggregates and the hydrated cement paste (Mehta and Monteiro 1997). Tensile strength of concrete typically ranges from 7% to 27% of its compressive strength for normal weight concrete (the higher the compressive strength, the lower the % of tensile strength), depending upon grade of concrete, water/cement ratio, curing age and size and type of aggregates

used (Mehta and Monteiro 1997). (iv) the strains in radial and circumferential directions are equal and due to this a unit outward radial displacement causes  $2\pi$  times elongation in circumference at the inner surface of cylinder and may get concentrated at the critical section depending upon the reinforcing bar position in concrete. If reinforcing steel bar is situated in symmetric environment, concrete will crack along one hazardous direction that will be chosen by the system.

Liu and Weyers model for time to crack cover concrete from corrosion initiation assumes the rate of steel mass loss caused by corrosion to decrease as time or thickness of corrosion product progresses (Liu 1996, Liu and Weyers 1998). Time to crack cover concrete from corrosion initiation predicted using this model is much larger as compared with their experimental observed values and thus over estimates or for the same experimental observed cracking time underestimates the steel loss. The time to crack cover concrete is predicted for experimental observed mass loss (Liu 1996, Liu and Weyers 1998) using the non-linear models from literature (Liu 1996, Liu and Weyers 1998, Kapilesh, Ghosh, Yasuhiro and Ramanujam 2006) are presented in the Table 5.

Kapilesh *et al.* (Kapilesh, Ghosh, Yasuhiro and Ramanujam 2006) derived the coefficient related to the rate of steel loss in Liu-Weyers model based on the best linear fit in experimental observed data (Liu 1996, Liu and Weyers 1998). Deviation of -4 to 66% from experimental observed time to crack cover concrete is observed and is as shown in Table 5. In formulations, the displacement of cracked concrete (material between inner radius and crack front) and displacement of crack front is assumed in proportion to the ratio of inner radius to radius at crack front i.e., the displacement at inner radius is smaller than displacement at crack front and thickness of cracked concrete is increased. This may not be possible as concrete is subjected to compressive stresses in radial direction and if any circumferential tensile stresses exist it will cause reduction in thickness of cracked concrete. Corrosion product characteristics  $\alpha=0.61309$  and  $\alpha_1=3.39357$  are estimated by carrying out regression using the experimental data in Table 1 (Liu 1996, Liu and Weyers 1998) (for different corrosion products) and used in their analytical predictions. But the predicted value of  $\alpha=0.61309$  and  $\alpha_1=3.39357$  possibly are not consistent with each other.

Morinaga 1988 proposed an empirical equation based on field and laboratory data to predict time to crack cover concrete. Time to crack cover concrete from corrosion initiation is assumed as function of corrosion rate, concrete cover and diameter of reinforcing steel bar only and ignores the mechanical properties of concrete which significantly affects the time to crack cover concrete.

This paper attempts to formulate a simple mathematical model to reasonably predict weight loss of reinforcing bar and time to concrete cover cracking in the corroded concrete structures. The proposed model is fully based on thick-walled cylinder approach. Analysis is carried out with and without considering the stiffness provided by the combination of the reinforcement and expansive corrosion products. The performance of the model is evaluated through the capability of reproducing the experimental trends and providing the reasonable estimates of the time to cover cracking. A sensitivity analysis has been carried out to show the influence of the various model input parameters. The proposed models evaluate the required radial displacement of inner surface of intact concrete to propagate the radial splitting cracks. The consistent displacement at inner surface of concrete is determined by preserving the volume of cracked concrete and is used to evaluate the mass loss of reinforcing bar. From known corrosion rate and estimated mass loss, the required time to crack cover concrete from onset of corrosion on reinforcing steel bar is predicted.

Table 1 Ratios  $\alpha$  and  $\alpha_1$  for various corrosion products [\*]

Corrosion products	FeO	Fe <sub>3</sub> O <sub>4</sub>	Fe <sub>2</sub> O <sub>3</sub>	Fe(OH) <sub>2</sub>	Fe(OH) <sub>3</sub>	Fe(OH) <sub>3</sub> ·3H <sub>2</sub> O
$\alpha$	0.777	0.724	0.699	0.622	0.523	0.347
$\alpha_1$	1.70	2.00	2.10	3.60	4.00	6.20
$M_w$ (g)	71.9	231.55	159.7	89.85	106.85	160.9

$\alpha$  is the ratio of molecular weight of iron to the molecular weight of corrosion products;  $\alpha_1$  is the ratio of volume of expansive corrosion products to the volume of iron consumed in the corrosion process;  $M_w$  is the molecular weight of corrosion product. [\*] Liu and Weyers 1998, Pantazopoulou and Papoulia 2001

## 2. Analytical modeling of corrosion cracking of concrete cover

### 2.1 Problem definition

Corrosion of steel is a process of oxidation and takes place in the presence of moisture and oxygen, resulting in formation of expansive corrosion products (rust) of smaller mass densities than original steel. Depending on the level of oxidation this rust occupy up to about 6.5 times the original iron volume consumed in the corrosion process creates tensile stresses in the surrounding concrete (Liu 1996, Mehta and Monteiro 1997, Liu and Weyers 1998). Some of the characteristic physical properties of corrosion products are as shown in Table 1 (Mehta and Monteiro 1997, Liu and Weyers 1998, Pantazopoulou and Papoulia 2001). Initially, before onsets of corrosion on steel rebar the concrete cylinder and the steel rebar will be in unrestrained condition and is as shown in Fig. 1(a). After filling the porous zone around the steel rebar by expansive corrosive products (unrestrained condition for steel rebar and expansive corrosion products, Fig. 1(b)) the inner surface of the concrete cylinder is displaced to accommodate the further production of expansive corrosion products (concrete cylinder subjected to internal radial pressure and in restrained condition, Fig. 1 (c)) depending on the level of oxidation. The steel bar surrounded by a rust layer after corrosion is as shown in Fig. 1(d). The internal pressure increases with the growth of corrosion products causing displacement of inner surface of concrete to accommodate the expansive corrosion products and increase in the tensile stresses in circumferential direction in concrete. When stiffness of steel and corrosion product is considered reinforcing steel and corrosion products combine would be subjected to an equivalent external pressure under equilibrium conditions. This will cause the reduced outward movement of the concrete (causes reduction in thickness of rust). When the tensile stresses in concrete reaches the cracking tensile strength of concrete, cracking at the inner surface of concrete occurs. This unidirectional stress field is reasonable as: (i) radial stress which is always compressive remains equal to internal pressure at inner surface of concrete and is numerically always less than the circumferential stress which is always tensile and is maximum at inner surface of concrete, (ii) the tensile strength of concrete is typically ranges from 7% to 27% of its corresponding compressive strength (Frederic and Patrick 2000). At this stage concrete can be represented in two zones cracked and un-cracked (intact/structural). Cracked concrete transfer the internal pressure by bearing to the inner surface of intact concrete (crack front) and will not carry any circumferential stresses. The intact concrete is subjected to tensile stresses less than the tensile strength of concrete and posses increased stiffness (as thickness of intact concrete decreases). As corrosion progresses the internal pressure builds-up causing increase in tensile stresses in intact

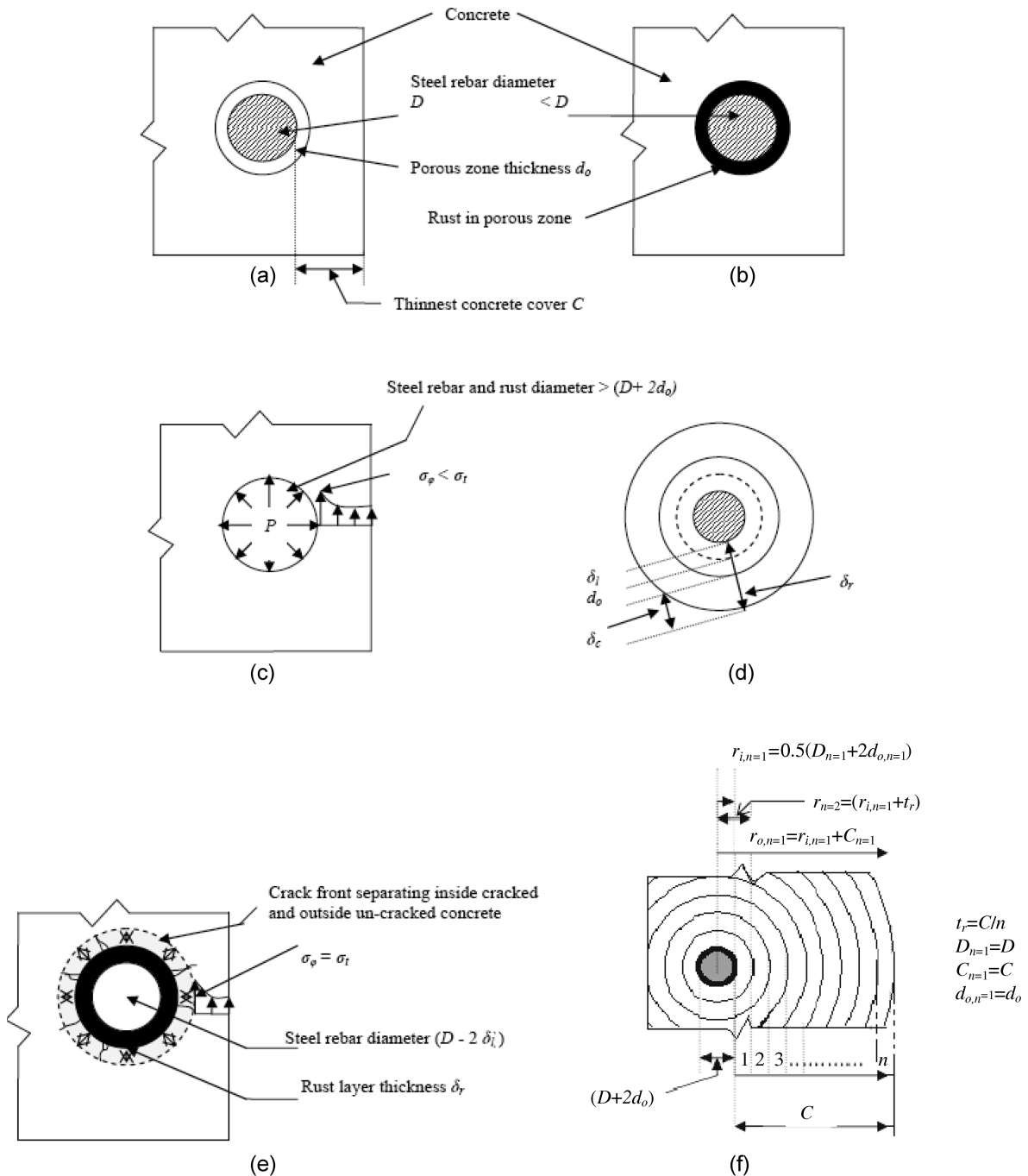


Fig. 1 (a) Initial unstrained condition for surrounding concrete and steel rebar; (b) Unstrained condition for surrounding concrete and steel rebar; (c) Concrete subjected to internal radial pressure in restrained condition; (d) Steel rebar surrounded by a rust layer after corrosion; (e) Propagation of radial splitting cracks from inner surface of concrete (crack front) due to corrosion process in progress; concrete at crack front is subjected to internal pressure and steel bar and rust combine is subjected to external pressure; (f) Division of cover and various terms involved in cracking analysis of first ring.

concrete, displacement of inner surface of concrete for preserving the volume and outward propagation of crack when tensile stress is reached/exceeded the tensile strength of concrete. Propagation of radial splitting cracks from inner surface of concrete due to corrosion process in progress is as shown in Fig. 1(e). Once the crack reaches concrete surface the concrete cover is assumed fully cracked. Proposed model has been developed assuming zero residual strength of cracked concrete and propagation of the radial smeared cracking of cover concrete based fully on thick-walled cylinder approach. The actual circumferential strain over the perimeter is obtained by summation of the discrete crack openings.

## 2.2 Basic assumptions

The following general assumptions are made in the proposed analytical model while formulating the corrosion-cracking model to determine the time for concrete cover cracking due to steel reinforcement corrosion:

(i) Although the real problem is three dimensional one, as the sum of radial and circumferential stresses remains constant, so that the deformation of all elements in the direction of the axis of the cylinder is the same and assuming cross sections of the cylinder remain plane after deformation, a two-dimensional approach is proposed, (ii) The buildup of the corrosion products over the reinforcement is spatially uniform, resulting in the uniform steel-concrete interface pressure due to expansive corrosion products, (iii) Corrosion rate is known in advance, (iv) the stresses produced are due to expansion of corrosion products only, (v) properties of concrete are time-independent, (vi) thickness of porous zone around the steel rebar is uniform, (vii) all corrosion products contribute equally in rust formation. (viii) Corrosion products shall also be accommodated within the open radial cracks during the progress of the crack front.

## 2.3 Mathematical formulations and estimating constants

### 2.3.1 Internal radial pressure caused by corrosion and cracking of concrete (Thick-wall cylinder approach)

Assuming the problem to be a plane stress (zero longitudinal stress), for a thick-walled cylinder of intact concrete of inner radius  $r_i$  and outer radius  $r_o$  the circumferential stress  $\sigma_\theta$  at a radius  $r$ , induced due to internal pressure  $p$  by expansive corrosion products is given by Eq. (1) (Timoshenko and Goodier 1970, Sadhu Singh 1981).

$$\sigma_\theta = \frac{p}{\left[1 - \left(\frac{r_i}{r_o}\right)^2\right]} \cdot \left[\left(\frac{r_i}{r_o}\right)^2 + \left(\frac{r_i}{r}\right)^2\right] \quad (1)$$

Rearranging the Eq. (1), the required internal radial pressure ( $p_{req}$ ) induced by corrosion products for cracking of concrete cover at inner radius  $r_i$  can be determined by equating the circumferential stress  $\sigma_\theta$  to tensile strength of concrete  $\sigma_t$  and is given by Eq. (2).

$$p_{req} = \sigma_t \cdot \left[\frac{(r_o^2 - r_i^2)}{(r_i^2 + r_o^2)}\right] \quad (2)$$

The radial stress ( $\sigma_r$ ) at any radius  $r$  is given by the Eq. (3). At the inner surface of intact concrete radial stress is equal to the internal radial pressure and is zero at the outer surface of concrete

cylinder.

$$\sigma_r = \left( \frac{r_i^2 \cdot P}{(r_o^2 - r_i^2)} \right) \cdot \left( 1 - \frac{r_o^2}{r^2} \right) \quad (3)$$

### 2.3.2 Flexibility constant ( $k$ )

The concrete displacement  $\delta_c$  caused due to  $p_{req}$  necessary to accommodate the expansive corrosion products is given by Eq. (4).

$$\delta_c = k \cdot p_{req} = \left[ \frac{r_i}{E_{ef}} \cdot \left( \frac{r_i^2 + r_o^2}{r_o^2 - r_i^2} + \nu_c \right) \right] \cdot p_{req} \quad (4)$$

where,  $k$  is the flexibility constant which relates the radial displacement to the internal radial pressure acting on the thick wall intact concrete cylinder (Stephen Timoshenko, 2002),  $E_{ef}$  is the effective modulus of elasticity of concrete and is equal to  $E_c/(1 + \phi_{cr})$  where,  $\phi_{cr}$  is the creep coefficient of concrete and  $\nu_c$  is the Poisson's ratio of concrete.

The flexibility  $k$  is bounded by infinite space ( $r_o = r_i + \infty$ ) from one side and by thick-wall cylinder (finite space) from other side ( $r_o = r_i + C$ ), where  $C$  is the thinnest intact concrete cover. The flexibility  $k$  can be obtained for infinite space and finite space as defined in Eq. (4) and their average  $k_{avg}$  is given by Eq. (5). The  $k_{avg}$  is used in the analysis. Considering, steel rebar of diameter  $D$ , thickness of porous zone around steel rebar  $d_o$ , we get  $r_i = (D + 2d_o)/2$ .

$$k_{avg} = (r_i/E_{ef}) \cdot [1 + \nu_c + (r_i^2/(C^2 + 2 \cdot C \cdot r_i))] \quad (5)$$

### 2.3.3 Displacement of concrete due to expansive corrosion products at inner surface of intact concrete ( $\delta_c$ )

A uniform corrosion of steel rebar in concrete causes uniform layer of corrosion products and would create uniform radial compressive stresses at the interface between steel rebar and concrete that results in a uniform radial displacement at the surface of the rust layer. The displacement of concrete necessary to reach the cracking stress/strength of concrete at the inner intact surface is given by Eq. (6).

$$\delta_c = P_{req} \cdot k_{avg} \quad (6)$$

### 2.3.4 Proposed equation for mass loss of steel reinforcing bar ( $M_{loss}$ )

Corrosion causes the reduction in original diameter of steel rebar ( $2 \cdot \delta_i$ ), development of rust, filling of the porous zone around the steel rebar and development of the internal radial pressure ( $p$ ). The internal radial pressure ( $p$ ) causes the displacement of concrete ( $\delta_c$ ) and propagates cracking at the inner surface of intact concrete depending on the position of rebar in concrete and when  $P$  reaches  $P_{req}$ . The porous zone around the steel rebar is assumed of uniform thickness equal to  $d_o$ . Thus the rust layer of thickness ( $\delta_r$ ) is produced around the steel rebar. Due to the formation of rust layer the original diameter of steel rebar ( $D$ ) reduces to  $(D - 2 \cdot \delta_i)$  and combined diameter of steel rebar and rust layer increases to  $[D + 2(\delta_r - \delta_i)]$ . For a unit length of steel rebar difference between volume of rust produced ( $V_r$ ) and volume of steel consumed ( $V_{sti}$ ) should be equal to the sum of difference in areas given by combined diameter of steel rebar and rust, and area of original steel rebar ( $D$ ) and the area of radial cracks ( $A_{rc}$ ); and is expressed by Eq. (7).

$$V_r - V_{sti} = [(M_r/\rho_r) - (M_{loss}/\rho_{st})] = (\pi/4) \cdot [\{D + 2(\delta_r - \delta_i)\}^2 - D^2] \quad (7)$$

where,  $M_r$  is the mass of rust per unit length of rebar,  $M_{loss}$  is the mass of steel consumed per unit

length of rebar to produce  $M_r$ ,  $\rho_r$  and  $\rho_{st}$  are the mass densities of rust and steel respectively. The thickness of rust,  $\delta_r = \delta_l + \delta_c + d_o$ ; the Eq. (7) can be expressed by Eq. (8).

$$[(M_r/\rho_r) - (M_{loss}/\rho_{st})] = (\pi/4) \cdot [\{4D \cdot (d_o + \delta_c) + 4(d_o + \delta_c)\}^2] \quad (8)$$

Neglecting the term,  $4 \cdot (d_o + \delta_c)^2$  as  $(d_o + \delta_c)^2 \ll D$ , the Eq. (8) can be expressed by Eq. (9).

$$[(M_r/\rho_r) - (M_{loss}/\rho_{st})] = \pi \cdot D \cdot (d_o + \delta_c) \quad (9)$$

Using the relationship,  $M_{loss} = \alpha \cdot M_r$  and  $\rho_r = \rho_{st} / (\alpha \cdot \alpha_1)$  in Eq. (9); the equation for the mass loss of steel per unit length ( $M_{loss}$ ) is proposed and is given by Eq. (10).

$$M_{loss} = \frac{\pi \cdot D \cdot \rho_{st} \cdot (d_o + \delta_c)}{(\alpha_1 - 1)} \quad (10)$$

If mass of the steel rebar diameter  $D$  is  $M_{stl}$  per unit length, then the reduced steel rebar diameter  $D_b$  can be determined by using Eq. (11)

$$D_b = \sqrt{4 \cdot (M_{stl} - M_{loss}) / (\pi \cdot \rho_{st})} \quad (11)$$

The reduction in diameter of steel rebar is given by Eq. (12)

$$\delta_l = 0.5 \cdot (D - D_b) \quad (12)$$

### 2.3.5 Estimation of characteristics of corrosion product $\alpha$ and $\alpha_1$

Due to lack of knowledge towards chemical composition and properties of the corrosion products in the case of corrosion affected reinforced concrete structures the characteristics of corrosion product  $\alpha$  is estimated by taking average of all corrosion products. Referring Table 1 the average value of  $\alpha$  is 0.615333. A closure value  $\alpha = 0.61309$  is obtained by other researcher (Kapilesh, Ghosh, Yasuhiro and Ramanujam 2006). The value  $\alpha = 0.615333$  lies in between 0.622 and 0.523. The  $\alpha_1$  value for  $\alpha = 0.615333$  is determined by linear interpolation between respective values of  $\alpha_1$  for  $\alpha = 0.622$  and 0.523. The estimated value of  $\alpha_1$  is 3.627. The product of  $\alpha$  for  $\alpha_1$  is equal to 2.232 and is in between 2 and 4 (Liu and Weyers 1998, Andrade, Alonso and Molina 1993).

### 2.3.6 Proposed equation for time to crack concrete cover from corrosion initiation

For a unit corrosion density  $i_{cor}$  in  $\mu A/cm^2$  the corrosion rate in  $mg/mm^2 \cdot day$  will be given by Eq. (13)

$$Corrosion\ rate = \frac{Corrosion\ current\ density}{n_c \cdot F} = 0.000864 \cdot \left( \frac{M}{n_c \cdot F} \right) = \frac{1}{4000} \quad (13)$$

where,  $M$  is the atomic mass of the metal (55.85 gm for Fe),  $n_c$  is the ionic charge ( $n_c = 2$  assuming all corrosion product is  $Fe(OH)_2$ ),  $F$  is the Faraday's constant (96494 A.s) and 0.000864 is the conversion constant. For  $\alpha = 0.615333$  the ionic charge lies between 2 and 3 and the weighted average value of 2.067 is proposed. For a known mass loss of steel rebar in  $mg/mm^2$  the time required to crack the concrete cover from corrosion initiation ( $T_{cr}$ ) in years is proposed and is given by Eq. (14).

$$T_{cr} = 11.328 \left( \frac{M_{loss}}{i_{cor}} \right) \quad (14)$$

## 2.4 Determination of the time to cover cracking from onset of corrosion on steel rebar

### 2.4.1 Formulation 1 (F-1)

The proposed analytical model is based on a thick-walled cylinder approach. In this formulation additional assumption is, strain in steel and rust combine is neglected (without considering the stiffness of corroded steel reinforcing bar) (Liu 1996, Liu and Weyers 1998, Tamer and Khaled 2007). A porous zone of assumed uniform thickness  $d_o$  around the steel rebar is shown in Fig. 1(a). The volume increase due to corrosion products creates internal pressure on the surrounding concrete after it occupies the porous zone around the steel reinforcing bar. The internal pressure increases with the growth of corrosion products causing displacement of inner surface of concrete to accommodate the expansive corrosion products and increase in the tensile stresses in circumferential direction in concrete. The analysis considers the propagation of radial splitting cracks gradually from inner surface of intact concrete to outer surface at thinnest concrete cover. In the analysis, thinnest concrete cover is divided into  $n$  number of equal parts (forming imaginary number of rings passing through inner and outer points of the parts) depending upon the difference between radial stresses at inner surface of two successive inner rings at a time when  $P$  reaches  $P_{req}$  (given by Eq. 2). Division of cover and various terms involved in cracking analysis of first ring are shown in Fig. 1(f). The radial stress at the inner surface of the second ring is calculated by using Eq. (3) and at the inner surface of second ring it is given by Eq. (15).

$$\sigma_{r,n=2} = \left( \frac{r_i^2 \cdot P_{req}}{r_o^2 - r_i^2} \right)_{n=1} \cdot \left( 1 - \frac{r_{o,n=1}^2}{r_{n=2}^2} \right) \quad (15)$$

where,  $\sigma_r$  is the radial stress,  $n$  indicates the number of ring and  $r$  is the inner radius of the ring where radial stress is to be determined (in Eq. (15) at  $n=2$ ). More the number of rings less will be the difference between radial stresses at inner surface of successive rings at a time. For first ring the radius of crack front is equal to the radius of inner surface of concrete. When  $P$  reaches  $P_{req}$  crack initiates at inner surface of first ring and it is assumed that crack is propagated up to the outer surface of inner ring. Stiffness is provided by full thickness of cover concrete before cracking of first ring and is determined by Eq. (5). Displacement at inner surface of first ring is determined by using Eq. (6).  $M_{loss}$ ,  $D_b$ , and  $\delta_l$  is calculated using Eqs. (10), (11), and (12). The thickness of rust  $\delta_r$  when cracking is initiated in the first ring is determined by summing respective values for  $d_o$ ,  $\delta_c$ , and  $\delta_i$ .

The analysis is repeated for cracking of second ring. The reduced diameter of steel rebar and thickness of rust layer after cracking of first ring will be considered as the original diameter of steel rebar and thickness of porous zone around the steel rebar respectively for the analysis of second ring i.e.,  $D_{n=2} = D_{b,n=1}$  and  $d_{o,n=2} = \delta_{r,n=1}$ . Now the concrete can be represented as cracked and uncracked/intact/structural. Circumferential stresses in the first ring are assumed to be relaxed due to cracking, but remaining concrete will be in strained condition and carries radial and circumferential stresses. The radial stress available ( $P_{avl, n=2}$ ) at inner surface of second ring when first is cracked can be determined by using Eq. (15), thus  $P_{avl} = \sigma_{r,n=2}$ . As crack front is moved concrete cover thickness reduces, inner and outer radius of intact concrete will change and requires to be considered in calculation of  $P_{req}$ ,  $K_{av}$ . The radius of concrete at interface of rust ( $R_{i,n=2}$ ), at inner ( $r_{i,n=2}$ ) and outer radius ( $r_{o,n=2}$ ) of intact concrete are given by Eqs (16), (17), and (18) respectively. Displacement at the inner surface of second ring is given by Eq. (19) and the displacement at interface of rust and concrete ( $d_{c,n=2}$ ) is given by Eq. (20).

$$R_{i,n=2} = 0.5(D_{n=2} + 2 \cdot d_{o,n=2}) \quad (16)$$

Let,  $t_r$  be the thickness of ring, then  $t_r = (C/n)$

$$r_{i,n=2} = R_{i,n=2} + (t_r \cdot (n-1)) \quad (17)$$

the intact thickness of concrete for the analysis to crack the concrete at second ring is  $C_{n=2} = C_{n=1} - t_r$ , therefore,

$$r_{o,n=2} = r_{i,n=2} + C_{n=2} \quad (18)$$

$$\delta_{c,n=2} = (P_{req,n=2} - P_{avl,n=2}) \cdot k_{avg} \quad (19)$$

$$d_{c,n=2} = \left( \frac{R_c}{R_f} \right)_{n=2} \cdot \delta_{c,n=2} \quad (20)$$

$M_{loss}$ ,  $D_b$ , and  $\delta_l$  is calculated using Eqs. (10), (11), and (12). The thickness of rust  $\delta_r$  when cracking is initiated in the second ring is determined by summing respective values for  $d_o$ ,  $\delta_c$ , and  $\delta_l$ .

The procedure of second ring is repeated till crack front (inner radius of intact concrete) reaches the inner surface of last ring. Time to crack cover concrete from corrosion initiation time is predicted from Eq. (14) for the  $M_{loss}$  calculated in the analysis of last ring and known corrosion current density.

#### 2.4.2 Formulation 2 (F-2)

In this approach the stiffness of steel and rust combine (corroded steel bar) is considered i.e. strain in steel and rust combine is considered. The time to crack cover concrete from corrosion initiation is determined using net displacement of concrete following the procedure as in (F-1). The additional assumptions considered are: i) poison's ratio of corrosion product is same as that of steel reinforcement, ii) Modulus of elasticity of steel and rust combine is equal to modulus of elasticity of un corroded steel. Due to expansive corrosion products the intact concrete at crack front is subjected to an internal pressure whereas the reinforcing steel and corrosion products combine would be subjected to an equivalent external pressure under equilibrium conditions. This will cause reduced outward movement of the interface between rust and concrete (causes reduction in thickness of rust). The combined diameter ( $D_c$ ) of the steel reinforcement plus the freely expanded corrosion products (rust layer) is obtained by using Eq. (21).

$$D_c = \sqrt{\left( \frac{4 \cdot (\alpha_1 - 1) M_{loss}}{(\rho_{st} \cdot \pi)} \right) + D^2} \quad (21)$$

The inward displacement ( $u$ ) of the combined diameter is calculated by using Eq. (22).

$$u = \frac{D_c \cdot R_c \cdot P_{req} \cdot (1 - \nu_s)}{2 \cdot r_i E_s} \quad (22)$$

Eq. (23) gives the net displacement and can be used to calculate the thickness of rust and  $M_{loss}$ .

$$\delta_{net} = d_c - u \quad (23)$$

### 3. Applications and performance of the model

#### 3.1 Numerical analysis

Apart from different experimental studies, different geometries and concrete properties; numerical analysis was carried out using formulations F-1 and F-2 for experimental data (Rasheeduzzafar, Al-saadoun and Al-Gahtani 1992, Liu 1996, Liu and Weyers 1998, Andres, Torres-Acosta and Alberto 2004). The time to crack concrete for these experimental studies ranges from hours to years and hence selected to compare the numerical analysis trend over a wider range. In the numerical analysis, the modulus of elasticity of concrete ( $E_c$ ) considering the type of aggregates used and mean value of the tensile strength of concrete ( $\sigma_t$ ) are determined as per recommendations of CEP-FIP model code (1990), average value of Poisson's ratio ( $\nu_c$ ) for concrete is taken as 0.15, creep coefficient ( $\Phi_{cr}$ ) for Liu-Weyers data is considered as 2.0 and for other researchers 3.1 (CEB-FIP 1990, Kapilesh, Ghosh, Yasuhiro and Ramanujam 2006) (considering dry atmospheric conditions as experiments are carried out in laboratory), the thickness of porous zone around steel rebar ( $d_o$ ) assumed is 12.5  $\mu\text{m}$ . The properties of steel considered in the analysis are density of steel ( $\rho_{st}$ ) as

Table 2 Experimental data and comparison of experimental and analytical predictions for slab and block specimen [\*].

SD	D	C	$i_{cor}$	$\sigma_c$	$M_{loss}$ (mg/mm <sup>2</sup> )				$T_{cr}$ (years)			
					[*]	[**]	Present work		[*]	[**]	Present work	
							F-1	F-2			F-1	F-2
S1	16	48	2.41	31.5	0.393	0.317	0.382	0.354	1.84	1.21	1.79	1.663
S2	16	70	1.79	31.5	0.601	0.584	0.683	0.629	3.54	5.56	4.32	3.978
S3	16	27	3.75	31.5	0.298	0.150	0.189	0.178	0.72	0.17	0.57	0.54
B1	12.7	52	1.8	31.5	0.392	0.427	0.497	0.466	2.38	3.72	3.13	2.93

[\*] Liu 1996, Liu and Weyers 1998, [\*\*] Kapilesh, Ghosh, Yasuhiro and Ramanujam 2006

Table 3 Experimental data and comparison of experimental and analytical predictions for CP specimen [\*\*\*]

SD	D	C	$i_{cor}$	$\sigma_c$	$X_{crit}$ (mm)				$T_{cr}$ (days)			
					[***]	[**]	Present work		[***]	[**]	Present work	
							F-1	F-2			F-1	F-2
CPB1	21	40.5	130	50	0.087	0.035	0.050	0.046	24	4.68	12.53	11.38
CPB2	21	40.5	110	50	0.068	0.035	0.050	0.046	20	5.53	14.57	13.45
CPC1	21	65.5	120	53	0.075	0.082	0.102	0.093	21	28.06	27.67	25.17
CPC2	21	65.5	140	53	0.120	0.082	0.102	0.093	28	24.05	23.72	25.58
CPD1	21	40.5	100	40	0.054	0.033	0.046	0.043	18	8.76	15.10	13.99
CPD2	21	40.5	100	40	0.069	0.033	0.046	0.043	20	5.5	15.10	13.99
CPF1	21	40.5	100	53	0.058	0.037	0.050	0.047	18	6.73	16.30	15.00
CPF2	21	40.5	120	53	0.063	0.037	0.050	0.047	17	5.61	13.59	12.51
CPG1	21	40.5	320	53	0.032	0.037	0.050	0.047	10	2.1	5.09	4.69
CPG2	21	40.5	190	53	0.062	0.037	0.050	0.047	10	2.1	8.58	7.90

[\*\*] Kapilesh, Ghosh, Yasuhiro and Ramanujam 2006, [\*\*\*] Andres, Torres-Acosta and Alberto 2004

78.6 KN/m<sup>3</sup>, Poisson's ratio for steel and rust combine ( $\nu_s$ ) as 0.3 and Modulus of elasticity ( $E_s$ ) as 210000 MPa. Characteristics of corrosion product  $\alpha$  and  $\alpha_1$  are taken as estimated in section 2.3.6. The thickness of equal parts/rings ( $t_r$ ) considered for all calculations is one mm. The experimental data (Rasheeduzzafar, Al-saadoun and Al-Gahtani 1992, Liu 1996, Liu and Weyers 1998, Andres, Torres-Acosta and Alberto 2004) and analytical predictions for  $M_{loss}$  and  $T_{cr}$  are as shown in Tables 2-4. In Tables 2-4, SD is specimen designation, and units for  $D$ ,  $C$ ,  $i_{cor}$  and  $\sigma_c$  are mm, mm,  $\mu\text{A}/\text{cm}^2$  and MPa. A sample calculation for first two rings and last ring using formulation F-2 for data of specimen S1 in Table 2 is presented in Table 5.

Table 4 Experimental data and comparison of experimental and analytical predictions for beam specimen [§]

SD	$D$	$C$	$i_{cor}$	$\sigma_c$	$M_{loss}$ (%)				$T_{cr}$ (Hours)			
					[§]	[**]	Present work		[§]	[**]	Present work	
							F-1	F-2			F-1	F-2
RB1	8	36.8	3000	35.4	2.75	2.719	3.387	3.286	60	31.11	17.61	17.09
RB2	12.7	31.75	3000	35.4	1.1	0.931	1.455	1.4	22.5	5.79	12.00	11.55
RB3	19	31.75	3000	35.4	0.5	0.474	0.803	0.76	14.5	2.24	9.92	9.41
RB4	38.1	24.1	3000	35.4	0.125	0.127	0.258	0.243	5.5	0.323	6.40	6.02
RB5	9.5	31.75	3000	35.4	1.75	1.75*	2.295	2.22	35	15.30	14.17	13.75
RB6	25.4	31.75	3000	35.4	0.23	0.23*	0.539	0.506	7	0.71	8.90	8.36

\*assumed same as experimentally predicted.

[§] Rasheeduzzafar, Al-saadoun and Al-Gahtani 1992, [\*\*] Kapilesh, Ghosh, Yasuhiro and Ramanujam 2006

Table 5 Sample calculation using formulation F-2 for specimen S1 in Table 2

Term	Unit	Equation used	1 <sup>st</sup> ring	2 <sup>nd</sup> ring	48 <sup>th</sup> ring
$\sigma_i, E_c$	MPa	CEB-FIP, 1990	3.047, 28365	3.047, 28365	3.047, 28365
$D$	mm	16mm	16	15.988	15.91
$d_o$	mm	0.0125mm	0.0125	0.0213	0.1179
$R_i$	mm	Eq. (16)	8.0125	8.0153	8.0733
$r_i$	mm	Eq. (17)	8.0125	9.0153	55.073
$C_n$	mm	for $n > 1$ ; $C_n = C_{n-1} - t_r$	$C_1 = C = 48$	47	1
$r_o$	mm	Eq. (18)	56.01	56.02	56.07
$P_{req}$	MPa	Eq. (2)	2.925	2.893	0.0548
$P_{avl}$	MPa	Eq. (15)	0.000	2.205	0.0537
$k_{avg}$	mm <sup>3</sup> /N	Eq. (5)	0.001	0.0011	0.1657
$\delta_c$	mm	Eq. (6, 19)	0.0029	0.0008	0.0002
$d_c$	mm	Eq. (20)	0.0029	0.0009	0.0012
$M_{loss}$	mg/mm	Eq. (10)	2.316	3.333	17.82
$D_b$	mm	Eq. (11)	15.988	15.983	15.909
$d_l$	mm	Eq. (12)	0.006	0.0026	0.0007
$D_c$	mm	Eq. (21)	16.031	16.044	16.235
$u$	mm	Eq. (22)	8E-5	9E-5	1E-5
$\delta_{net}$	mm	Eq. (23)	0.0028	0.0008	0.0012
$\delta_r$	mm	$(d_o + \delta_{net} + d_l)$	0.0213	0.0247	0.1198
$T_{cr}$	years	Eq. (14)		1.663	

### 3.2 Numerical analysis for $T_{cr}$ only

A separate analysis is carried out to see the performance of Eq. (14) proposed for determination of time to crack cover concrete from corrosion initiation time. Time to crack cover concrete ( $T_{cr}$ ) is determined using proposed Eq. (14) using experimental data of corrosion current density and observed mass loss (Liu 1996, Liu and Weyers 1998), results of the proposed analysis were compared with the experimental observations (Liu 1996, Liu and Weyers 1998) and analytical predictions (Liu 1996, Liu and Weyers 1998, Kapilesh, Ghosh, Yasuhiro and Ramanujam 2006) and are presented in Table 6. Analytical predictions of Liu-Weyers model are very much away from the experimental observations and hence in Table 6 the % deviation is not calculated. The variation of  $T_{cr}$  in years with  $(M_{loss}/i_{cor})$  in  $mg/mm^2$  per  $\mu A/cm^2$  is demonstrated in Fig. 2.

### 3.3 Sensitivity analysis

The various parameters involved in the analysis of time to cover cracking due to steel rebar corrosion in reinforced concrete structures are: diameter of steel rebar, uniaxial compressive strength of concrete, the interrelating constants for tensile strength and modulus of elasticity with uniaxial compressive strength of concrete (if data for tensile strength and modulus of elasticity is not

Table 6 Comparison of experimental and analytically predicted values of  $T_{cr}$  for experimental observed values of  $M_{loss}$  for slab and block specimen [\*]

Experimental observed			Model predicted $T_{cr}$ (years)					
Reference [*]			Reference [*]		Reference [**]		Present work	
$M_{loss}$ ( $mg/mm^2$ )	$i_{cor}$ ( $\mu A/cm^2$ )	$T_{cr}$ (years)	$\alpha=0.523$	$\alpha=0.622$	$\alpha=0.61309$	% deviation	$\alpha=0.615$	% deviation
0.298	3.75	0.72	13.471	11.33	0.69	-4.1	0.900	25.03
0.393	2.41	1.84	36.457	30.65	1.87	1.57	1.847	0.39
0.392	1.80	2.38	61.182	51.44	3.36	41.2	2.467	3.65
0.601	1.79	3.54	114.79	96.52	5.88	66.2	3.803	7.44
Average deviation in % from experimental observed $T_{cr}$						26.23		9.13

[\*] Liu 1996, Liu and Weyers 1998, [\*\*] Kapilesh, Ghosh, Yasuhiro and Ramanujam 2006

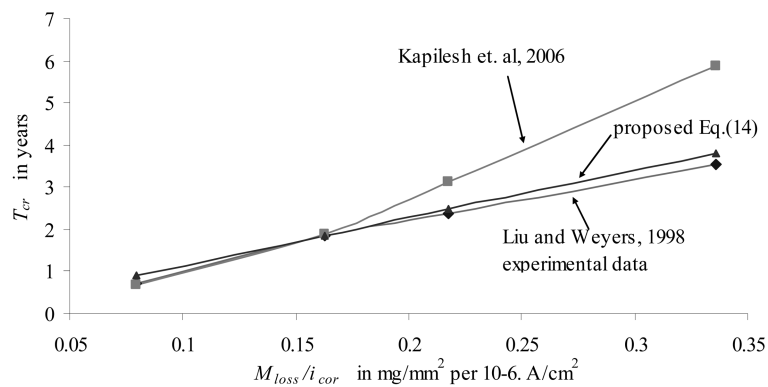


Fig. 2 Variation of  $T_{cr}$  as a function of  $(M_{loss}/i_{cor})$

available), creep of concrete, Poisson's ratio of concrete, thickness of porous zone around the steel rebar, clear cover to reinforcement, characteristics of corrosion products, and corrosion current density. The material strength in the actual structure may be different than the considered design strength depending upon quality control on ingredients, workmanship and curing methods and periods.

In the proposed sensitivity analysis, the important variables in the proposed model are varied over a wide range depending upon different codes specification, literature information and using formulation F-1 and F-2. Only one parameter was varied at a time and the other parameters were kept at their reference value for specimen designation S1 in Table 2 (Data as reported in the reference literature (Liu 1996, Liu and Weyers 1998). The following variables are considered:

1. Thickness of porous zone ( $d_o$ ) have been varied from 10 to 20  $\mu\text{m}$  (Thoft-Christensen 2000, Tamer and Khaled 2007).
2. Poisson's ratio ( $\nu_c$ ) has been varied from 0.1 to 0.2 (CEB-FIP 1990).
3. Creep coefficient ( $\Phi_{cr}$ ) has been varied from 1 to 3.1 (CEB-FIP 1970, CEB-FIP 1990).
4. Different inter-relations of  $\sigma_t$  with  $\sigma_c$  give large variation in values of  $\sigma_t$  for same compressive strength of concrete, hence in the same analysis if inter-relation is changed it will affect the predicted  $T_{cr}$ , to know the effect of this the tensile strength ( $\sigma_t$ ) of the concrete has been varied from 2 to 5.5 MPa for  $\sigma_c=31.5$  MPa (ACI 318-1985, CEB-FIP 1990, IS 456-2000, Frederic and Patrick 2000).
5. Different inter-relations of  $E_c$  with  $\sigma_c$  give variation in values of  $E_c$  for same compressive strength of concrete, hence in the same analysis if inter-relation is changed it will affect the predicted  $T_{cr}$ , to know the effect of this the modulus of elasticity of concrete ( $E_c$ ) has been varied from 25 to 31 GPa for  $\sigma_c=31.5$  MPa (ACI 318-1985, CEB-FIP1970, Canadian Standards Association A23.3-94-1994, IS 456-2000).
6. As per code specifications for concrete the tensile strength ( $\sigma_t$ ) and modulus of elasticity ( $E_c$ ) are functions of compressive strength ( $\sigma_c$ ). The compressive strength of concrete has been varied from 20 to 80 MPa. Two cases are considered separately: Case 1:- tensile strength ( $\sigma_t$ ) (Carasquillo, Nilson and Slate, 1981, Frederic and Patrick, 2000) and modulus of elasticity ( $E_c$ ) (CSA, 1994) are square root functions of compressive strength ( $\sigma_c$ ) and the relationship considered is, Case 2:- tensile strength ( $\sigma_t$ ) and modulus of elasticity ( $E_c$ ) are other than square root functions of compressive strength ( $\sigma_c$ ) and the relationship considered is (CEB-FIP, 1990),

$$\sigma_t = 0.94\sqrt{\sigma_c} \text{ and } E_c = 4500\sqrt{\sigma_c}$$

7. The variation on  $T_{cr}$  is observed for the mass loss predicted by the model using base values; corrosion current density is varied from 0.5 to 10  $\mu\text{A}/\text{cm}^2$  (Andrade, Alonso and Molina 1993).
8. Ratio of molecular weight of iron to the molecular weight of corrosion product  $\alpha$ , has been varied from 0.622 to 0.523 i.e.,  $n_c=2$  to 3.

In order to know the effect in general on  $T_{cr}$  the following parameters are varied over a wider range:

9. Diameter of the reinforcing bar ( $D$ ) has been varied from 8 to 25 mm i.e.,  $C/D$  ratio varied from 6 to 1.92.
10. Clear cover of concrete to the reinforcing bar ( $C$ ) has been varied from 25 mm to 75 mm.
11. Modulus of elasticity of reinforcing steel rebar has been varied from 1,00,000 to 2,50,000 Mpa. Corroded steel bar (steel bar with rust combine) posses lesser modulus of elasticity hence larger deviation of  $E_s$  on lower side is considered.

3.4 Discussion of results

For the experimental observed  $M_{loss}$  data (Liu 1996, Liu and Weyers 1998) in Table 6, the  $T_{cr}$  predicted using the proposed model (Eq. (14)) are in good agreement with experimental observations of  $T_{cr}$ . The experimental observed  $T_{cr}$ , analytical prediction of Kapilesh, Ghosh, Yasuhiro and Ramanujam 2006 and predicted by Eq. (14) for the experimental data of Liu 1996, Liu and Weyers 1998 are represented in Fig. 2.

The results of the numerical analysis with formulations F-1 and F-2 for the experimental studies (Rasheeduzzafar, Al-saadoun and Al-Gahtani 1992, Liu 1996, Liu and Weyers 1998, Andres, Torres-Acosta and Alberto 2004) are compared with the respective experimental observations and analytical predictions (Kapilesh, Ghosh, Yasuhiro and Ramanujam 2006) and presented in Tables 2-4. The results compared are for the mass loss and time to crack concrete from corrosion initiation. For the considered data the formulation F-1 overestimates up to about 7% than formulation F-2. The proposed model results are in good agreement with the experimental observations than reported in the reference Kapilesh, Ghosh, Yasuhiro and Ramanujam 2006.

Variation of  $T_{cr}$  with thickness of porous zone ( $d_o$ ) is demonstrated in Fig. 3.  $T_{cr}$  increases with the increasing porous zone thickness uniformly and about 12.6% for formulation F-1 and 13.66% for formulation F-2 increase is found for the considered range of  $d_o$ . More the thickness of porous zone more will be the required quantity of rust to fill it and thus it keeps the cover concrete in unstressed condition for longer period. More the metal loss more will be the  $T_{cr}$  required. In actual more  $d_o$  is not desirable because this may result in more section loss of steel reinforcement without or showing corrosion signs at later stage on concrete surface.

The variation of  $T_{cr}$  with Poisson's ratio ( $\nu_c$ ) is demonstrated in Fig. 4.  $T_{cr}$  increases with the increasing Poisson's ratio uniformly by about 5 to 5.5%. Creep coefficient depends upon the exposure conditions of the member.

$T_{cr}$  increases with the increasing creep coefficient ( $\Phi_{cr}$ ) uniformly as shown in Fig. 5 and an increase of 80.54% for formulation F-1 and 90.46% for formulation F-2 is observed over the lower value considered. Lower the relative humidity higher will be the  $\Phi_{cr}$ . (CEB-FIP 1970, CEB-FIP 1990, Mehta and Monteiro 1997). Higher the value of  $\Phi_{cr}$  more will be the  $k_{avg}$  and can sustain more displacement of concrete due to rust before cover cracking.

The effects of using different inter-relations of  $\sigma_t$  with  $\sigma_c$  give large variation in values of  $T_{cr}$  for

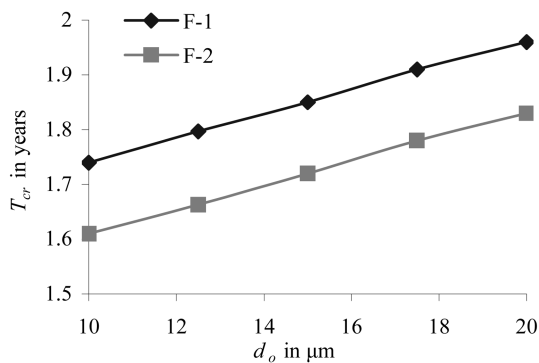


Fig. 3  $T_{cr}$  as a function of  $d_o$ , for specimen S1 (Table 2)

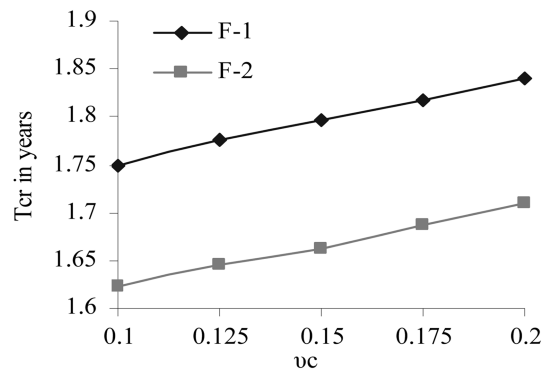


Fig. 4  $T_{cr}$  as a function of  $\nu_c$ , Specimen S1 (Table 2)

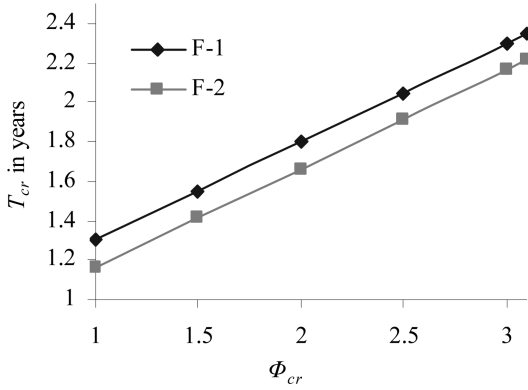


Fig. 5  $T_{cr}$  as a function of  $\Phi_{cr}$ , Specimen S1 (Table 2)

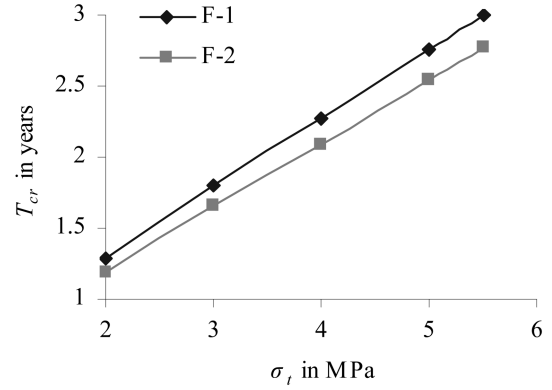


Fig. 6  $T_{cr}$  as a function of  $\sigma_t$ , Specimen S1 (Table 2)

same compressive strength of concrete. Maintaining same value for modulus of elasticity of concrete and other parameters, uniform increase up to 134% of  $T_{cr}$  with increasing  $\sigma_t$  from 2 to 5.5 MPa has been found for both the formulations. The variation of  $T_{cr}$  as a function of  $\sigma_t$  is demonstrated in Fig. 6.

The effects of using different inter-relations of  $E_c$  with  $\sigma_c$  shows a variation up to about 18 to 20% in predicted values of  $T_{cr}$  for the same compressive strength of concrete using both the formulations. The variation of  $T_{cr}$  with  $E_c$  is as demonstrated in Fig. 7.

For concrete the tensile strength ( $\sigma_t$ ) and modulus of elasticity ( $E_c$ ) are functions of compressive strength ( $\sigma_c$ ):

Case 1: When tensile strength ( $\sigma_t$ ) and modulus of elasticity ( $E_c$ ) are square root functions of compressive strength ( $\sigma_c$ ) the  $\delta_c$  given by Eq. (6) will remain same for any value of compressive strength of concrete and hence  $T_{cr}$  will not change. Thus for square root inter-relationships  $T_{cr}$  is dependant on ratio of coefficient for tensile strength to coefficient for modulus of elasticity (0.94/4500) and does not vary with compressive strength of concrete.

Case 2: For the relationship of tensile strength ( $\sigma_t$ ) and modulus of elasticity ( $E_c$ ) other than square root functions of compressive strength ( $\sigma_c$ ), the variation of  $T_{cr}$  with  $\sigma_c$  is demonstrated in

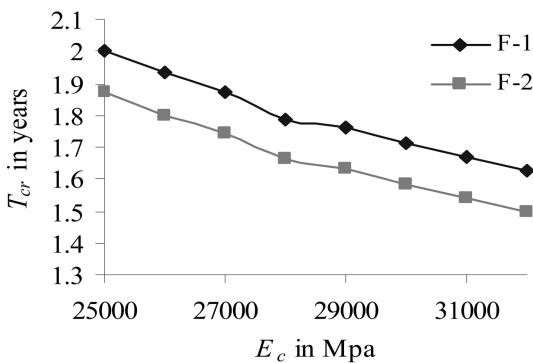


Fig. 7  $T_{cr}$  as a function of  $E_c$ , Specimen S1 (Table 2)

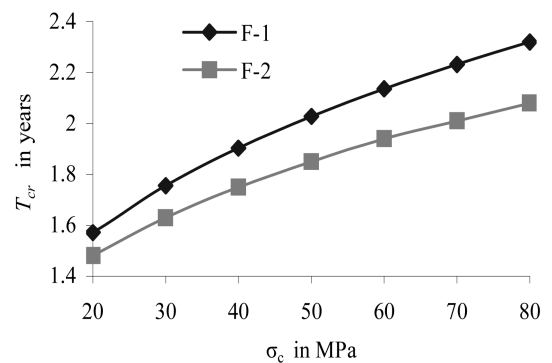


Fig. 8  $T_{cr}$  as a function of  $\sigma_c$ , Specimen S1 (Table 2)

Fig. 8. About 47% and 40% increase of  $T_{cr}$  had been found over lower considered value of compressive strength using formulation F-1 and F-2 respectively.

$T_{cr}$  decreases following power variation by about 95% when the corrosion current density ( $i_{cor}$ ) is varied from 0.5 to 10  $\mu\text{A}/\text{cm}^2$  for the mass loss predicted by the model using base values and its variation is represented in Fig. 9. In a given time mass loss increases with corrosion current density ( $i_{cor}$ ).

For the considered data when corrosion product is assumed as  $\text{Fe}(\text{OH})_2$  the mass loss will be increased by 24.5% and  $T_{cr}$  will be reduced by 17% as compared with the values when corrosion product assumed is  $\text{Fe}(\text{OH})_3$ . The variation is demonstrated in Fig. 10.

Increasing the diameter of steel reinforcing bar by keeping all other parameters same  $T_{cr}$  decreases and mass loss per unit length increases or per unit area and in % decreases. The variation of  $T_{cr}$  and % mass loss using formulation F-1 is demonstrated in Fig. 11. Relation between  $T_{cr}$  and diameter is found to be,  $T_{cr} = 9.5761.D^{-0.5972}$  with  $R^2 = 0.9964$ .  $T_{cr}$  uniformly increases with increasing C/D ratio. Increasing the concrete cover to the reinforcing bar keeping all other parameters same, will increase the  $T_{cr}$  and also mass loss per unit length or in % or per unit area.

The variation of  $T_{cr}$  with modulus of elasticity is demonstrated in Fig. 12. As corrosion progresses

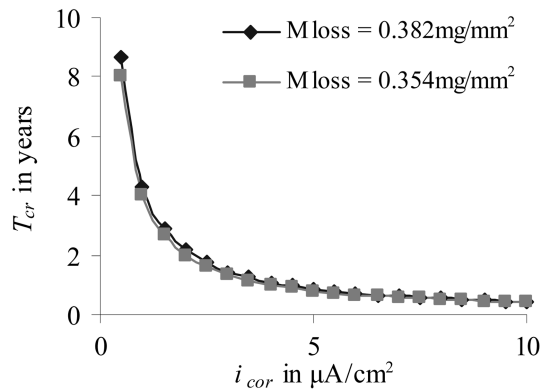


Fig. 9  $T_{cr}$  as a function of  $i_{cor}$ , Specimen S1 (Table 2)

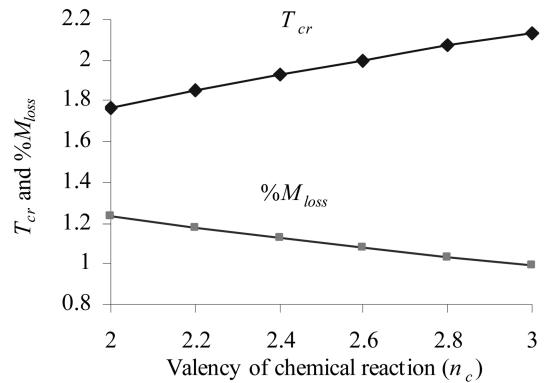


Fig. 10  $T_{cr}$  and %  $M_{loss}$  as a function of  $n_c$ , Specimen S1 (Table 2), Formulation F-1

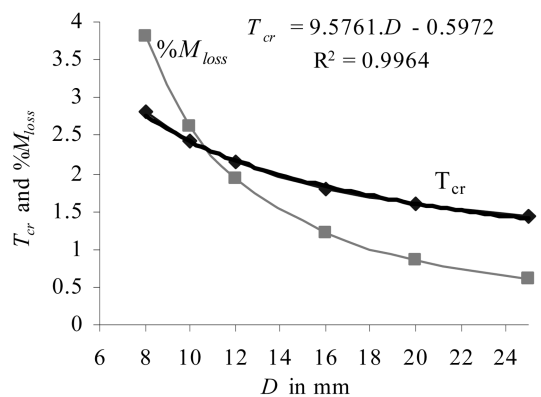


Fig. 11  $T_{cr}$  and %  $M_{loss}$  as a function of  $D$ , for specimen S1 (Table 2), Formulation F-1

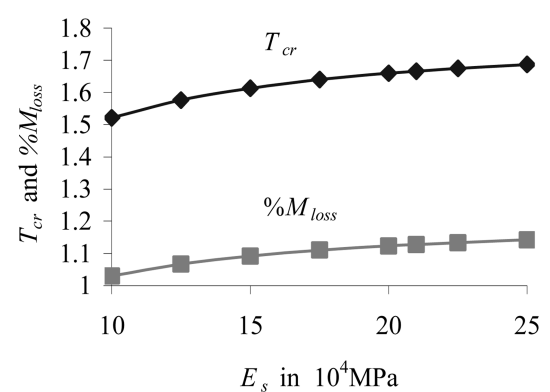


Fig. 12  $T_{cr}$  and %  $M_{loss}$  as a function of  $E_s$ , for specimen S1 (Table 2), Formulation F-2

rust formation will be more, which reduces the modulus of elasticity of steel bar and rust combine. Lower the modulus of elasticity lower will be the  $T_{cr}$  keeping all other parameters same. This gradual decrease of modulus of elasticity is required to be considered in the analysis of  $T_{cr}$ . An increase in  $T_{cr}$  up to about 11% is found over the considered lower value of  $E_s$ . % mass losses will also follow the similar trend to that of  $T_{cr}$ .

#### 4. Conclusions

The proposed linear model for time to crack cover concrete from corrosion initiation, predicts better results than other non linear analytical models for the considered experimental mass loss data. The proposed values of  $\alpha$  and  $\alpha_1$  in the analysis are consistent with each other.

Formulation F-1 and F-2 both reproduces equally the experimental trends. The formulation F-2 is better as it also considers the stiffness of corroded bar. The F-1 overestimates for  $M_{loss}$  and  $T_{cr}$  is up to 7% than F-2.

The cover cracking is mainly dependant on the selected material properties, inter-relations used, corrosion current density, and assumed corrosion product and their properties. The sensitivity analysis carried out in this paper is not useful for better formulation but it demonstrates how the parameter variation effects the time to cracking of cover concrete. The parameter variation ranges considered covered in general normal extremities. Similar sensitivity analysis may be carried out to study the  $T_{cr}$  variation with a particular parameter as it may be useful to improve the workmanship, to select the concrete grade, to decide the cover thickness and to select the bar diameter for a particular member at particular location. For predicting the tensile strength and modulus of elasticity of concrete from compressive strength; data base, methods used for testing, materials used in the region (ex. aggregate type, etc.) and basis used (mean or failure) is required to be studied to select the inter-relation i.e., one needs to be cautious to select the concrete tensile strength. Collection of the data base of properties of concrete manufactured using local material in the region may be useful in future. The variation of  $T_{cr}$  with  $\sigma_c$  is useful in deciding the concrete grade.  $i_{cor}$  depends upon the available favorable conditions for the corrosion. For a reinforced concrete member of particular grade in service the parameter variation will remain small and probabilistic methods can be used to study the combined effect of all parameters on  $T_{cr}$ . Better formulation shall produce the experimental trend or service behavior of member as it increases the efficiency of timely measures taken for corrosion protection.

From the sensitivity analysis for the considered ranges of the parameters, the most sensitive variables in descending order are tensile strength of concrete, corrosion current density, creep coefficient of concrete, compressive strength of concrete, assumed corrosion product, modulus of elasticity of concrete, thickness of porous zone, modulus of elasticity of steel rebar and rust combine and Poisson's ratio of concrete.

Increasing the diameter of steel reinforcing bar by keeping all other parameters same  $T_{cr}$  decreases and mass loss per unit length increases or per unit area and in % decreases.  $T_{cr}$  uniformly increases with increasing C/D ratio. Lower the value of modulus of elasticity of steel rebar or steel rebar and rust combine, lower will be the time to crack cover concrete ( $T_{cr}$ ) from onset of corrosion. The gradual decrease of modulus of elasticity of corroding steel rebar is required to be considered in the analysis of  $T_{cr}$ .

In the proposed model the area of radial cracks is considered by reducing the thickness of cracked

concrete (more displacement at the concrete inner surface than at crack front) for volume preservation indicates that corrosion products are assumed to accommodate fully within the radial cracks; in actual practice this quantity may be less. To quantify this aspect and in particular, the possible convection of the corrosion products experimentation would be required. The average value of the  $\alpha$  for corrosion product is considered, which is close to the corrosion product  $\text{Fe}(\text{OH})_2$ , if actual corrosion product is different the values of  $M_{\text{loss}}$  and  $T_{\text{cr}}$  will be different.

The present study for time to cover cracking from onset of corrosion may be useful in making certain cost-effective decisions pertaining to the monitoring inspections and control of corrosion, repair of RC member/structure in corrosive environment

## References

- ACI 318 (1985), "Standard code requirements for reinforced concrete and commentary", *Am. Conc. Inst.*, Detroit, USA.
- Andrade, C., Alonso, C., and Molina, F. J. (1993), "Cover cracking as a function of bar corrosion: Part 1- experimental test", *Mater. Struct.*, **26**, 453-464.
- Andres, A. Torres-Acosta and Alberto A. Sagues (2004), "Concrete cracking by localized steel corrosion- Geometric effects", *ACI Mater. J.*, **101**(6), 501-507.
- Canadian Standards Association, (CSA) A23.3-94 (1994), *Design of Conc. Struct.*, Canadian Standards Association, Rexdale, ON, Canada.
- Carasquillo, R.L., Nilson, A.H., and Slate, F.O. (1981), "Properties of high-strength concrete subjected to short-term loads", *ACI J. Proceedings*, **78**(3), 171-178.
- CEB-FIP (1970), *International Recommendations for the Design and Construction of Concrete Structures*.
- CEB-FIP (1990), *Comite Euro-International du Beton-Federation International de la Precontrainte-Design Code*, London (UK): Thomas Telford.
- Frederic Legeron and Patrick Paultre (2000), "Prediction of modulus of rupture of concrete", *ACI Mater. J.*, **97**(2), 193-200.
- IS 456 (2000), "Indian standard code of practice for plain and reinforced concrete", 4<sup>th</sup> revision, Bureau of Indian standards, New Delhi, India
- Kapilesh Bhargava, A.K. Ghosh, Yasuhiro, and Mori, S. Ramanujam (2006), "Model for cover cracking due to rebar corrosion in RC structures", *Eng. Struct.*, **28**, 1093-1109.
- Liu, Y. (1996), "Modeling the time to corrosion cracking of the cover concrete in chloride contaminated reinforced concrete structures", *Dissertation, at Virginia polytechnic Institute and State University*, Blacksburg, VA., October.
- Liu, Y. and Weyers, R.E. (1998), "Modeling the time-to-corrosion cracking in chloride contaminated reinforced concrete structures", *ACI Mater. J.*, **95**(6), 675-681.
- Mehta, P.K. and Monteiro, P.J.M. (1997), *Concrete Microstructure, Properties and Materials*, 1<sup>st</sup> edition, Chennai (India); Indian concrete Institute.
- Morinaga, S. (1988), "Prediction of service lives of reinforced concrete buildings based on rate of corrosion of reinforcing steel", *Report No. 23*, Shimizu Corp. Japan, 82
- Pantazopoulou, S.J. and Papoulia, K.D. (2001), "Modeling cover-cracking due to reinforcement corrosion in RC structures", *J. Eng. Mech.*, **127**(4), 342-351.
- Rasheeduzzafar, Al-saadoun S.S. and Al-Gahtani, A.S. (1992), "Corrosion cracking in relation to bar diameter, cover and concrete quality", *J. Mater. Civil Eng.*, ASCE, **4**(4), 327-343.
- Sadhu Singh (1981), *Theory of Plasticity*. 1<sup>st</sup> edition, Khanna Publishers, Delhi (India).
- Stephen Timoshenko (2002), *Strength of Materials Part II Advanced theory and Problems*, 3<sup>rd</sup> edition, CBS publishers and distributors, New Delhi (India)
- Tamer KI Maaddawy and Khaled Soudki (2007), "A model for prediction of time from corrosion initiation to corrosion cracking", *Cement Concrete Compo.*, **29**(3), 168-175.

- Timoshenko, S.P. and Goodier, J.N. (1970), *Theory of Elasticity*, 3<sup>rd</sup> ed. New York (USA): McGraw-Hill Book Co.
- Thoft-Christensen P. (2000), "Stochastic modeling of the crack initiation time for reinforced concrete structures", *ASCE Struct. Congress*, Philadelphia, May 8-10, 8.